

Enhanced  $B(E3)$  strength observed in  $^{137}\text{La}$ 

Md. S. R. Laskar<sup>1</sup>, R. Palit<sup>1</sup>, E. Ideguchi<sup>2</sup>, T. Inakura<sup>3</sup>, S. N. Mishra,<sup>1,4</sup> F. S. Babra,<sup>1</sup> S. Bhattacharya,<sup>5</sup> D. Choudhury<sup>6</sup>, Biswajit Das<sup>1</sup>, B. Das<sup>1</sup>, P. Dey,<sup>1</sup> U. Garg<sup>7</sup>, A. K. Jain,<sup>8</sup> A. Kundu,<sup>1</sup> D. Kumar,<sup>9</sup> D. Negi<sup>10</sup>, S. C. Pancholi<sup>10</sup>, S. Rajbanshi,<sup>11</sup> and S. Sihotra<sup>9</sup>

<sup>1</sup>Department of Nuclear and Atomic Physics, Tata Institute of Fundamental Research, Mumbai 400005, India

<sup>2</sup>Research Center for Nuclear Physics (RCNP), Osaka University, Ibaraki, Osaka 567-0047, Japan

<sup>3</sup>Laboratory for Advanced Nuclear Energy, Tokyo Institute of Technology, Meguro, Tokyo 152-8550, Japan

<sup>4</sup>Indian Institute of Science Education and Research, Berhampur-760010, India

<sup>5</sup>Department of Pure & Applied Physics, Guru Ghasidas Vishwavidyalaya, Koni, Bilaspur 495009, India

<sup>6</sup>Department of Physics, Indian Institute of Technology, Ropar, Punjab 140001, India

<sup>7</sup>Physics Department, University of Notre Dame, Notre Dame, Indiana 46556, USA

<sup>8</sup>Amity Institute of Nuclear Science & Technology, Amity University, Noida 201301, UP, India

<sup>9</sup>Department of Physics, Panjab University, Chandigarh 160014, India

<sup>10</sup>Inter University Accelerator Centre, New Delhi-110067, India

<sup>11</sup>Department of Physics, Presidency University, Kolkata-700073, India



(Received 9 April 2021; accepted 9 July 2021; published 22 July 2021)

The  $^{137}\text{La}$  nucleus was populated by the reaction  $^{130}\text{Te}(^{11}\text{B}, 4n)$  at 40-MeV beam energy and the lifetime of the  $11/2^-$  state at 1004.6 keV was measured using a hybrid array of HPGe clover and  $\text{LaBr}_3(\text{Ce})$  detectors by electronic fast-timing technique, providing the value  $T_{1/2} = 263 \pm 12$  ps. The reduced transition probability  $B(E3) = 23.3 \pm 2.4$  W.u. is found to be significantly larger compared to the values observed in lighter odd- $A$  La isotopes. The experimentally determined  $B(E3)$  value is compared with theoretical calculations of random-phase approximation which explains the enhanced transition probability to be arising from higher contribution of the  $g_{9/2}$  orbital to the proton transition density.

DOI: [10.1103/PhysRevC.104.L011301](https://doi.org/10.1103/PhysRevC.104.L011301)

One of the prominent themes of nuclear structure physics is the investigation of the effects of octupole correlations on the low-lying excitations in nuclei [1,2]. The coupling of single-particle and octupole degrees of freedom enriches the complexity in the level structure and remains a subject of contemporary interest [3,4]. A recent theoretical investigation has predicted several regions of ground-state octupole deformation across the nuclear landscape [5]. The region of Ba, Ce, Nd, and Sm isotopes around  $^{146}\text{Ba}$  is reported to constitute the second-largest concentration of octupole unstable nuclei predicted theoretically that are within the experimental range. Ba isotopes are preferred for studying octupole correlations due to the gap in proton single-particle levels at  $Z = 56$  for  $\beta_3 = 0.1$  [6]. The presence of strong octupole correlations in this region has been confirmed by studies of even-even isotopes, in which negative-parity bands have been observed at lower excitation energy and connected to the positive-parity ground-state bands by strong electric dipole transitions. Interestingly, more distinctive signatures of octupole deformation are expected in odd- $A$  isotopes. Therefore, the predicted gap in proton levels for octupole deformed  $Z = 56$  nuclei should make Cs and La isotopes good candidates for observing parity doublets. While neutron-rich Cs isotopes did not show any enhanced octupole correlation,  $^{145}\text{La}$  isotope showed similar enhancement compared to  $^{144}\text{Ba}$  [7]. In addition, the  $B(E3)$  transition strengths are a good measure for the octupole col-

lectivity, and the systematics of experimental  $B(E3; 3^- \rightarrow 0^+)$  strengths for even-even nuclei across the landscape have been described in Ref. [8].  $B(E3)$  strengths for transition other than  $3^- \rightarrow 0^+$  have also been studied recently in mass 50, and 210 regions [9,10]. In particular, the  $B(E3; 3^- \rightarrow 0^+)$  values of the chain of even-even Ba isotopes starting from  $^{132}\text{Ba}$  to  $^{138}\text{Ba}$  [11] and  $^{144}\text{Ba}$  to  $^{146}\text{Ba}$  [12,13] indicate substantial octupole collectivity in these nuclei. Recently, the neighboring odd-mass  $^{143}\text{Ba}$  has been studied to investigate the interplay between single-particle and collective octupole degrees of freedom [14]. An upper limit on lowest  $E3$  matrix element was reported for  $^{143}\text{Ba}$  from this Coulomb excitation experiment which suggests that the static octupole deformation may not provide the right description for  $^{143}\text{Ba}$  and implies instead a dynamic nature. Therefore, it is interesting to see the similar evolution in odd- $A$  La isotopes and how it compares to the even-even Ba isotopes. For some of the lighter La isotopes, the  $B(E3)$  from  $11/2^-$  to  $5/2^+$  state are reported to have smaller values compared to the neighboring even-even Ba isotopes [15]. The present study aims to extract the  $B(E3)$  in  $^{137}\text{La}$  from lifetime measurement for understanding the evolution of octupole collectivity in the La isotopes.

The excited states of  $^{137}\text{La}$  were populated through the fusion evaporation reaction  $^{130}\text{Te}(^{11}\text{B}, 4n)$  at a beam energy of 40 MeV. The  $^{11}\text{B}$  projectile, obtained from the Pelletron Linac Facility at the Tata Institute of Fundamental Research

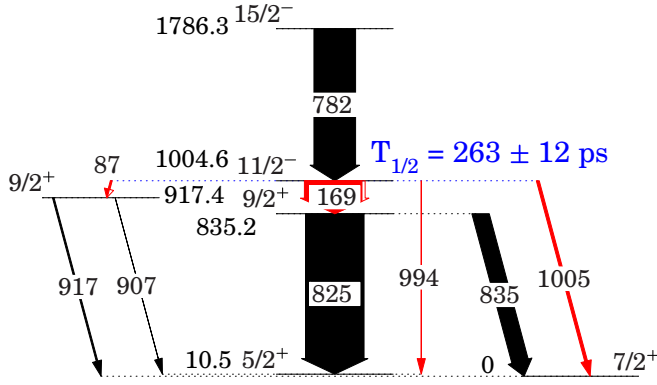


FIG. 1. Partial level scheme of  $^{137}\text{La}$  relevant for this work. Numbers on the left of each level show the excitation energy in keV. Numbers in each arrow are the transition energy in keV and the thickness of the arrows are proportional to intensities. The transition energies shown in the level scheme have been rounded to the nearest whole numbers. Red line 87.2-, 169.4-, 993.7-, and 1004.6-keV  $\gamma$  rays have been used for evaluating branching ratio of 993.7-keV transition.

(TIFR), Mumbai, was incident on the 1.6-mg/cm<sup>2</sup>-thick  $^{130}\text{Te}$  target, evaporated on 5.5 mg/cm<sup>2</sup>  $^{197}\text{Au}$ . A hybrid array consisting of 11 Compton-suppressed high-purity germanium (HPGe) clover detectors arranged in spherical geometry and 14  $\text{LaBr}_3(\text{Ce})$  detectors coupled with digital data acquisition system [16] was used for the experiment. Four HPGe clover detectors were arranged in 90° (three in 140°, three in 157°, and one at 115°) with respect to the beam direction. To reduce the Compton continuum, each HPGe clover detector is shielded by BGO scintillation detector. The crystal of  $\text{LaBr}_3(\text{Ce})$  detectors were in cylindrical shape of  $\varnothing 2'' \times 2''$ . The full width at half maximum (FWHM) of  $\gamma$  rays at 1.33-MeV energy for the HPGe clover and  $\text{LaBr}_3(\text{Ce})$  detectors were  $\sim 2.4$  and 30 keV, respectively. A mixed source consisting of  $^{152}\text{Eu}$  and  $^{133}\text{Ba}$  isotopes, placed at the target position, was used for the energy calibrations of the HPGe clover and  $\text{LaBr}_3(\text{Ce})$  detectors. The time-stamped data were collected with two- and higher-fold coincidence condition using an XIA-based digital data-acquisition system [16]. Two crate synchronization method was used, with one crate for six digitizer modules with 100-MHz sampling frequency for HPGe clover and other for 1 module with 250-MHz sampling frequency for  $\text{LaBr}_3(\text{Ce})$  detectors. The details of the method will be communicated through a different paper [17]. The data were sorted using an offline analysis code “MultipARame-ter time-stamp-based COincidence Search program” [18] and RADWARE [19] to generate an NTuple containing coincident  $\gamma$  rays and the time differences between different detectors. The partial level scheme of  $^{137}\text{La}$  relevant for present discussion is shown in Fig. 1. The lifetime of 11/2<sup>-</sup> state in  $^{137}\text{La}$  was previously reported as an upper limit of  $T_{1/2} \leq 410(70)$  ps [20]. The  $\gamma$  rays decaying from the 11/2<sup>-</sup> state are marked as red in the level scheme and consistent with the Ref. [21], which reported a weak transition of 87.2 keV in addition to 169.4-, 993.7-, and 1004.6-keV transitions mentioned in the other earlier works on  $^{137}\text{La}$  [20,22,23]. We have

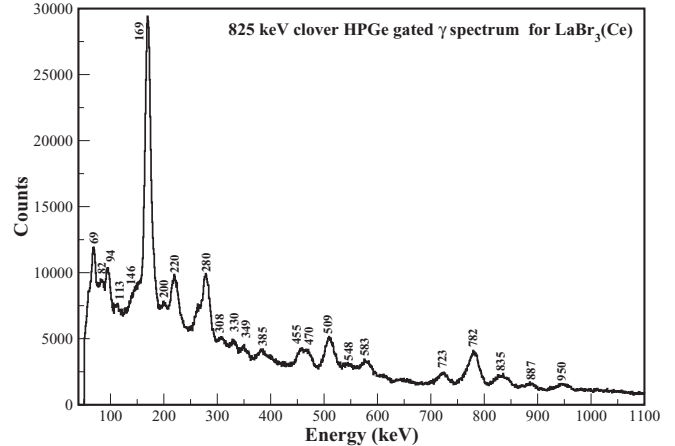


FIG. 2.  $\text{LaBr}_3(\text{Ce})$  energy spectrum obtained by gating on the 825-keV transition in the HPGe clover detectors.

remeasured the lifetime of this state in the present work using the hybrid array. Figure 2 shows a gated  $\gamma$ -ray spectrum observed in the  $\text{LaBr}_3(\text{Ce})$  detectors which was used to obtain the time differences across the 11/2<sup>-</sup> state in  $^{137}\text{La}$  at excitation energy of 1004.6 keV. The energy gate from the HPGe clover detectors has been used to select the cascade of  $\gamma$  rays across the 1004.6-keV state in  $\text{LaBr}_3(\text{Ce})$  to get the time spectrum. The decay half-lives for the states were extracted using time difference spectrum between any two transitions  $E_{\gamma 1}$  and  $E_{\gamma 2}$  in a cascade. The time difference spectrum can be obtained from the list mode data using the following procedure. Four conditional time spectra ( $T_{p1,p2}$ ,  $T_{p1,bg2}$ ,  $T_{bg1,p2}$ , and  $T_{bg1,bg2}$ ) were generated from the time-stamped data. Here  $T_{p1,p2}$  represents the time difference spectrum obtained with energy gate around the  $E_{\gamma 1}$  and  $E_{\gamma 2}$  peaks, while  $T_{p1,bg2}$  represents the same for energy gate around the  $E_{\gamma 1}$  peak and background near  $E_{\gamma 2}$  peak. Similarly, the third and fourth spectra are for background-peak and background-background spectra, respectively. Then the final time difference spectrum was generated by the following formula [16]:

$$T(i) = T_{p1,p2}(i) - T_{p1,bg2}(i) - T_{bg1,p2}(i) + T_{bg1,bg2}(i). \quad (1)$$

The fitting method incorporated the full response function of the time spectra which was assumed to be a convolution of a Gaussian prompt-response function (PRF) and a single component exponential decay associated with the state lifetime [24,25]. The convolution function associated with a single exponential decay, defined by a mean-lifetime of the decaying state,  $\tau = \frac{t_{1/2}}{\ln 2}$  and a Gaussian PRF defined by a standard deviation from the mean  $\sigma$ , where the FWHM for the Gaussian distribution is given by  $2.35\sigma$ , can be written as,

$$I(t) = A \exp\left(\frac{\sigma^2}{2\tau^2} - \frac{1}{\tau}\right) \left[1 - \text{erf}\left(\frac{\sigma^2 - \tau t}{\sqrt{2}\sigma\tau}\right)\right], \quad (2)$$

where erf() corresponds to the error function,  $A$  is an intensity normalization constant, and  $t$  is the time difference since the defined time zero. The time spectrum was fitted with exponential convoluted by Gaussian function. The method has been utilized recently in Ref. [26]. All the data fitting has been carried out using the ROOT software packages [27].

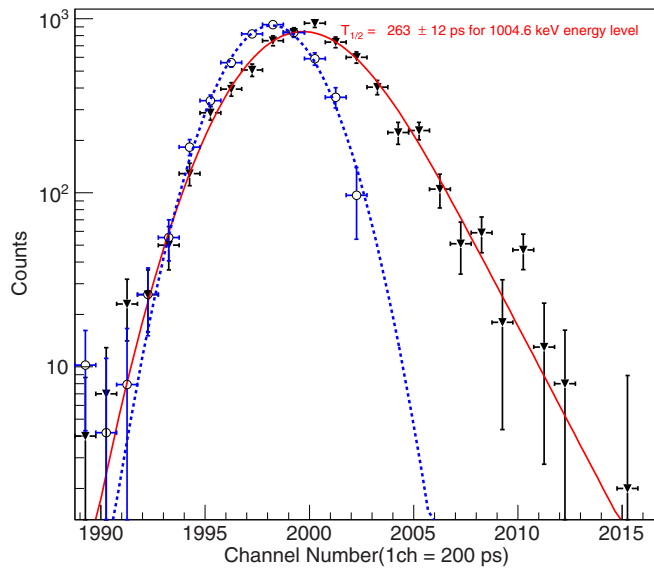


FIG. 3. Time difference spectrum (fitted with exponential convoluted by Gaussian function as represented by red color solid line) was depicted between  $\text{LaBr}_3(\text{Ce})$  detectors with  $\gamma$  gated on HPGe, while 169.4 keV at start, and 782 keV at stop in  $\text{LaBr}_3(\text{Ce})$ , showing  $T_{1/2} = 263 \pm 12$  ps for 1004.6-keV energy level. The prompt curve (fitted with Gaussian function as represented by blue color dashed line) having FWHM =  $985 \pm 23$  ps was generated with start at 94 keV and stop at 455 keV (not shown in Fig. 1) from  $^{137}\text{La}$  nucleus.

The half-life, on fitting the time spectrum with the function of Eq. (2) has been found to be  $263 \pm 12$  ps for the  $11/2^-$  state at an excitation energy of 1004.6 keV as shown in Fig. 3. The nature of  $\gamma$ -ray transition between  $11/2^-$  to  $5/2^+$  is  $E3$  type. For  $E3$  transition, the reduced transition probability is given by [28,29]

$$B(E3) = \frac{1.75 \times 10^{-3}(0.693)}{t_{1/2\text{partial}} E_\gamma^7} e^2 \text{ fm}^6. \quad (3)$$

For an isomeric state with  $N$  branches, predominantly  $\gamma$  rays and internal conversion in the present cases, the partial  $\gamma$ -ray mean life of an individual transition  $i$ ,  $\tau_\gamma^i = \tau_{\text{partial}}$  is given by [29]

$$\tau_{\text{partial}} = \tau_\gamma^i = \tau^{\text{exp}} \frac{\sum_{k=1}^N I_\gamma^k (1 + \alpha^k)}{I_\gamma^i} = \tau^{\text{exp}} / R_B \quad (4)$$

where  $\tau^{\text{exp}}$  is the experimental level mean life,  $I_\gamma^k$  ( $k = 1, 2, 3, \dots, N$ ) are the  $\gamma$ -ray intensities of the depopulating transitions,  $\alpha^k$  are the total conversion coefficients, and the branching ratio ( $R_B$ ) is given by the following equation,

$$R_B = \frac{I_\gamma^i}{\sum_{k=1}^N I_\gamma^k (1 + \alpha^k)}. \quad (5)$$

Consequently, the partial half-life becomes

$$t_{1/2\text{partial}} = 0.693 \tau_{\text{partial}} = T_{1/2}^{\text{exp}} / R_B \quad (6)$$

where  $T_{1/2}^{\text{exp}} = T_{1/2}$  is the measured half-life of the particular state.

TABLE I. Summary of intensities for different  $\gamma$  rays decaying from  $11/2^-$  state with 1004.6 keV. These values are used to calculate  $R_B$  of 993.7-keV transition.

$E_\gamma$ (keV)	Relative Intensity	$\alpha_{\text{tot}}$
87.2	$1.65 \pm 0.17$	0.034
169.4	$93.44 \pm 0.48$	0.055
993.7	$0.57 \pm 0.05$	0.004
1004.6	$4.82 \pm 0.05$	0.006

The corresponding single particle Weisskopf estimate for  $E3$  transition is [28]

$$B^W(E3) = 5.940 \times 10^{-2} A^2 e^2 \text{ fm}^6. \quad (7)$$

Using Eq. (5), and Table I, the branching ratio of 993.7-keV transition has been evaluated as  $[(5.4 \pm 0.5) \times 10^{-3}]$  to get the partial half-life of the  $11/2^-$  state. The 782.1-keV gated spectrum was used for finding the branching ratios of all the transitions decaying from the  $11/2^-$  state at 1004.6-keV excitation energy. While extracting the intensity of the 993.7-keV transition, the summing effect for the parallel cascade consisting of 169.4- and 824.8-keV transitions has been taken into account. The count in the peak of the 993.7-keV transition due to the summing of 169.4- and 824.8-keV transitions is estimated to be 0.11% of the yield of 169.4-keV transition based on the GEANT4 simulation results [30]. The GEANT4 estimate of the summing effect of the cascade of  $\gamma$  rays has been confirmed from the comparison of the area of the sum-peak of 169.4- and 782.1-keV transitions at 951.5 keV and the area of the 169.4-keV transitions in the 455.8-keV gated spectrum (see the level scheme given in Ref. [22]). The reduced transition probability using Eq. (3), and Eq. (6) for the 993.7-keV transition is found to be  $B(E3) = [(26.0 \pm 2.7) \times 10^3] e^2 \text{ fm}^6$ , which corresponds  $23.3 \pm 2.4$  W.u. in Weisskopf single-particle estimate.

The measured  $B(E3; 11/2^- \rightarrow 5/2^+)$  value in  $^{137}\text{La}$  has been compared with that of the same transitions in lighter odd- $A$  La isotopes wherever data are available in Fig. 4 [15]. In the same figure, the experimental  $B(E3; 3^- \rightarrow 0^+)$  values for even-even Ba isotopes were also plotted. The comparison of  $B(E3)$  values between even-even Ba and odd- $A$  La isotopes provides the systematics to understand the coupling between the particle and phonon states in this region. Reference [3] provides an overview of the recent experiments and theoretical attempts to understand low-energy spectra of odd- $A$  nuclei close to magic and semi-magic cores, where particle-phonon coupling phenomena play a significant role. The nuclei around  $^{48}\text{Ca}$ ,  $^{132}\text{Sn}$ ,  $^{208}\text{Pb}$ , and neutron-rich Ni isotopes were discussed. The behavior of  $B(E3)$  strengths for transition  $9/2^+ \rightarrow 3/2^-$  have been described in particle phonon coupling model in a chain of odd mass Cu (having one proton only outside the Ni closed shell) isotopes [3]. The significantly large  $E3$  strength for  $9/2^+$  states ( $\approx 20$  W.u.) in  $^{63}\text{Cu}$  and  $^{65}\text{Cu}$ , was attributed to the coupling with the  $3^-$  phonons of  $^{62}\text{Ni}$  [ $B(E3) = 13(2)$  W.u.] and  $^{64}\text{Ni}$  [ $B(E3) = 10(2)$  W.u.] [8], respectively. It will be an interesting case to see whether similar kind of behavior exists for the case

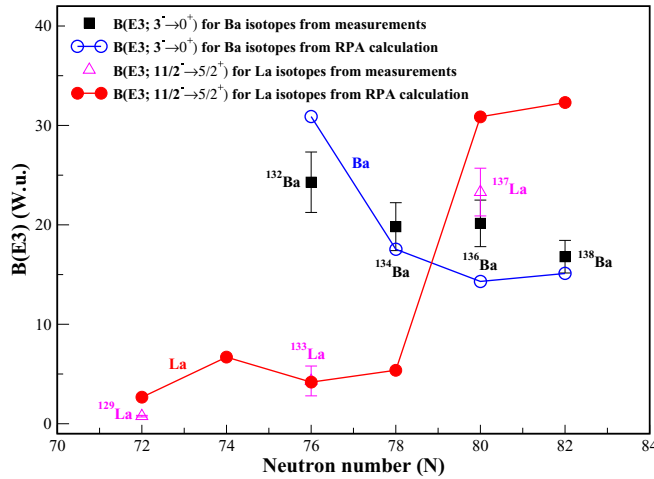


FIG. 4. Variation of experimental  $B(E3)$  strengths in Ba and La isotopes. The RPA results have been compared with the experimental data. The experimental  $B(E3; 11/2^- \rightarrow 5/2^+)$  of  $^{129,133}\text{La}$  isotopes from Ref. [15] and  $B(E3; 3^- \rightarrow 0^+)$  of  $^{132,134,136,138}\text{Ba}$  isotopes have been adopted from Ref. [11]. The  $B(E3; 11/2^- \rightarrow 5/2^+)$  of  $^{137}\text{La}$  is from present work. The experimental and theoretical values are overlapping for the  $^{133}\text{La}$  isotope.

of odd-mass La [ $B(E3); 11/2^- \rightarrow 5/2^+$ ] and even-mass Ba [ $B(E3); 3^- \rightarrow 0^+$ ] isotopes. Figure 4 shows that our measured  $B(E3)$  value in  $^{137}\text{La}$  is larger compared to  $B(E3)$  values for the same transition in the lighter odd- $A$  La isotopes [15]. It is important to notice that the  $B(E3; 11/2^- \rightarrow 5/2^+)$  value measured for  $^{137}\text{La}$  isotope with  $N = 80$  is comparable with the  $B(E3; 3^- \rightarrow 0^+)$  in  $^{136}\text{Ba}$ , an isotope of  $^{137}\text{La}$ , while that of  $^{133}\text{La}$  is much smaller compared to the  $B(E3; 3^- \rightarrow 0^+)$  of  $^{132}\text{Ba}$ .

To understand the experimental value of  $B(E3)$  strength, we have performed the random-phase approximation (RPA) calculation [31]. The static properties were obtained by a Hartree-Fock calculation. For describing the excited  $5/2^+$  state in  $^{137}\text{La}$ , we assume spherical symmetry and employ the filling approximation. Namely, 8 (6) protons with occupation probability 6/8 (1/6) occupy  $g_{7/2}$  ( $d_{5/2}$ ) orbit, respectively, and 12 neutrons with occupation probability 10/12 occupy  $h_{11/2}$  orbit. The RPA calculations with Skyrme SLY4 interaction [32] was applied to the  $5/2^+$  state in a self-consistent manner to calculate the properties of the excited  $11/2^-$  state. Figure 4 depicts the comparison of the measured  $B(E3; 3^- \rightarrow 0^+)$  of Ba isotopes and  $B(E3; 11/2^- \rightarrow 5/2^+)$  of La isotopes with the RPA results. The RPA calculations provide a good description of the variation of measured  $B(E3)$  values for even-even Ba isotopes and odd- $A$  La isotopes. Note that the calculation indicates a sudden increase of the  $B(E3)$  value at  $N = 80$  La isotope, which is even more than the  $B(E3; 3^- \rightarrow 0^+)$  in  $^{136}\text{Ba}$ , while those of  $N < 80$  stay much smaller values compared to the respective even-even Ba isotopes. Remarkably, the model explains the sudden rise of  $B(E3)$  value for  $^{137}\text{La}$  compared to the lighter La isotopes. It will be important to measure the  $B(E3)$  strengths in  $^{135}\text{La}$  and  $^{139}\text{La}$  isotopes to firmly establish the sudden rise of the  $B(E3)$  in La isotopes. The

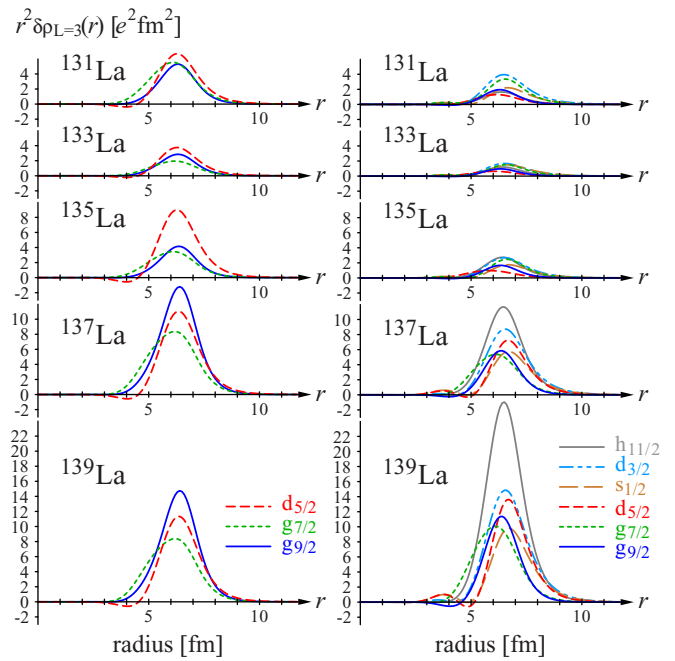


FIG. 5. Proton and neutron transition densities ( $r^2 \delta \rho_{L=3}$ ) decomposed to hole states. The gray solid line, cyan dashed double-dotted line, amber long-dashed line, red dashed line, green dotted line, and blue solid line are for  $h_{11/2}$ ,  $d_{3/2}$ ,  $s_{1/2}$ ,  $d_{5/2}$ ,  $g_{7/2}$ , and  $g_{9/2}$ , respectively.

proton and neutron transition densities of different states are calculated in the RPA to understand the variation of  $B(E3)$  values in La isotopes. Fig. 5 depicts the proton and neutron transition densities of excitations from  $5/2^+$  state to  $11/2^-$  state, decomposed to the hole orbitals in  $5/2^+$  states. It indicates that  $g_{9/2}$ ,  $g_{7/2}$ , and  $d_{5/2}$  proton orbits in  $5/2^+$  state are important for exciting to  $11/2^-$  state. As shown in Fig. 5, all decomposed transition densities have the same sign (positive), implying large coherency. This indicates that all  $11/2^-$  states have strong isoscalar nature. It is clearly seen that as moving from  $^{135}\text{La}$  to  $^{137}\text{La}$ , both proton and neutron transition densities are enhanced coherently. The calculated transition densities contribution of proton  $g_{9/2}$  (blue line) seems to be responsible for the sudden increase of  $B(E3)$  value for  $^{137}\text{La}$  isotope. In  $^{139}\text{La}$ , the proton transition densities are similar to those in  $^{137}\text{La}$ , while the neutron transition densities are furthermore enhanced. The sudden rise of  $B(E3)$  in  $^{137}\text{La}$  is explained by the activation of proton  $g_{9/2}$  orbit, which is induced by increasing of neutron number occupying  $h_{11/2}$  orbit. On the other hand, such enhancement is not seen in Ba isotopes. This study indicates the possibility of the role of unknown contribution of proton-neutron correlation on the evolution of  $B(E3; 11/2^- \rightarrow 5/2^+)$  strength in La isotopes which needs further exploration in future.

In summary, the lifetime of  $11/2^-$  state in  $^{137}\text{La}$  has been found to be  $263 \pm 12$  ps, which provides  $B(E3; 11/2^- \rightarrow 5/2^+)$  strength as  $23.3 \pm 2.4$  W.u. The present  $B(E3; 11/2^- \rightarrow 5/2^+)$  value of  $^{137}\text{La}$ , when compared with that of the lighter La isotopes, confirms for the first time a sudden increase of  $B(E3)$  strength at  $N = 80$ .

The nature of evolution of  $B(E3; 11/2^- \rightarrow 5/2^+)$  strength, which is a measure of octupole collectivity, in odd- $A$  La isotopes seems to be different from the  $B(E3; 3^- \rightarrow 0^+)$  of even-even Ba isotopes. These observed variations of  $B(E3)$  strengths for La and Ba isotopes have been well explained by RPA calculations. With the addition of an odd proton in  $d_{5/2}$  to the even-even Ba core, the evolution of octupole collectivity in La isotopes changes significantly with respect to that of the Ba isotopes. Experimentally it will be important to investigate the  $B(E3)$  strength for  $11/2^-$  to  $5/2^+$  transition in  $^{135}\text{La}$  and  $^{139}\text{La}$  isotopes to test the predictions of the present RPA calculations. These measurements are required to understand the dynamics of the interaction which causes the sudden rise of the proton  $g_{9/2}$  contribution in the transition densities near  $N = 82$ . This work suggests that the possible role of several  $\Delta L = 3$  couplings involving the various orbitals which are reinforcing each other needs to be explored.

Authors are grateful to the staff at TIFR-BARC Pelletron Linac Facility for providing good quality beam and smooth operation of the accelerator for the entire duration of the experiment. The help and cooperation from B. Naidu, S. Jadhav, Abraham T. Vazhappilly and R. Donthi for setting up the experimental apparatus is acknowledged. This work is supported by the Department of Atomic Energy, Government of India (Project Identification No. RTI 4002), and the Department of Science and Technology, Government of India (Grant No. IR/S2/PF-03/2003-II). U.G. acknowledges the U.S. National Science Foundation (Grants No. PHY-1713857 and No. PHY-2011890). R.P. and E.I. acknowledge the RCNP Collaboration Research network (COREnet) program. E.I. acknowledges KAKENHI Grant No. 17H02893 and the support by the International Joint Research Promotion Program of Osaka University. A.K.J. thanks SERB (Government of India) for a research grant. D.N. acknowledges CSIR, India.

---

[1] P. A. Butler and W. Nazarewicz, *Rev. Mod. Phys.* **68**, 349 (1996).

[2] L. M. Robledo and G. F. Bertsch, *Phys. Rev. C* **84**, 054302 (2011).

[3] S. Leoni, A. Bracco, G. Coló, and B. Fornal, *Eur. Phys. J. A* **55**, 247 (2019).

[4] K. Nomura, T. Niksic, and D. Vretenar, *Phys. Rev. C* **97**, 024317 (2018).

[5] Y. Cao, S. E. Agbemava, A. V. Afanasjev, W. Nazarewicz, and E. Olsen, *Phys. Rev. C* **102**, 024311 (2020).

[6] I. Ahmad and P. A. Butler, *Annu. Rev. Nucl. Part. Sci.* **43**, 71 (1993).

[7] W. Urban, W. R. Phillips, J. L. Durell, M. A. Jones, M. Leddy, C. J. Pearson, A. G. Smith, B. J. Varley, I. Ahmad, L. R. Morss, M. Bentaleb, E. Lubkiewicz, and N. Schulz, *Phys. Rev. C* **54**, 945 (1996).

[8] R. H. Spear, *At. Data Nucl. Data Tables* **42**, 55 (1989).

[9] D. Montanari *et al.*, *Phys. Lett. B* **697**, 288 (2011).

[10] D. Ralet *et al.*, *Phys. Lett. B* **797**, 134797 (2019).

[11] S. M. Burnett *et al.*, *Nucl. Phys. A* **432**, 51 (1985).

[12] B. Bucher, S. Zhu, C. Y. Wu, R. V. F. Janssens, D. Cline, A. B. Hayes, M. Albers *et al.*, *Phys. Rev. Lett.* **116**, 112503 (2016).

[13] B. Bucher, S. Zhu, C. Y. Wu, R. V. F. Janssens, R. N. Bernard, L. M. Robledo *et al.*, *Phys. Rev. Lett.* **118**, 152504 (2017).

[14] C. Morse, A. O. Macchiavelli, H. L. Crawford, S. Zhu, C. Y. Wu, Y. Y. Wang *et al.*, *Phys. Rev. C* **102**, 054328 (2020).

[15] Evaluated Nuclear Structure Data File (ENSDF).

[16] R. Palit, S. Saha, J. Sethi, T. Trivedi, S. Sharma, B. S. Naidu, S. Jadhav, R. Donthi, P. B. Chavan, H. Tan, and W. Hennig, *Nucl. Instrum. Methods Phys. Res. A* **680**, 90 (2012).

[17] Md. S. R. Laskar *et al.*, to be communicated.

[18] R. Palit and S. Saha, *Pramana* **82**, 649 (2014).

[19] D. C. Radford, *Nucl. Instrum. Methods Phys. Res. A* **361**, 306 (1995).

[20] J. R. V. Hise and G. Chilosi, *Phys. Rev.* **161**, 1254 (1967).

[21] E. A. Henry, N. Smith, P. G. Johnson, and R. A. Meyer, *Phys. Rev. C* **12**, 1314 (1975).

[22] S. Chanda, T. Bhattacharjee, S. Bhattacharyya, S. K. Basu, R. K. Bhowmik, S. Muralithar, R. P. Singh, B. Mukherjee, N. S. Pattabiraman, S. S. Ghugre, and M. B. Chatterjee, *Nucl. Phys. A* **775**, 153 (2006).

[23] M. L. Li, S. J. Zhu, S. D. Xiao, X. L. Che, Y. N. U, Y. J. Chen, H. B. Ding, L. H. Zhu, G. S. Li, S. X. Wen, and X. G. Wu, *Eur. Phys. J. A* **28**, 1 (2006).

[24] S. G. Malmskog, *Nucl. Phys.* **62**, 37 (1965).

[25] B. Olsen and L. Boström, *Nucl. Instrum. Methods* **44**, 65 (1966).

[26] L. A. Gurgi, P. H. Regan, T. Daniel, Z. Podolyák, A. M. Bruce, P. J. R. Mason, N. Mărginean, R. Mărginean, V. Werner, T. Alharb, N. Alkhomashi, A. D. Bajoga, R. Britton, I. Căta-Danil, R. J. Carroll, D. Deleanu, D. Bucurescu, N. Florea, I. Gheorghe, D. G. Ghita, T. Glodariu, R. Lice *et al.*, *Radiat. Phys. Chem.* **137**, 7 (2017).

[27] R. Brun and F. Rademakers, *Nucl. Instrum. Methods Phys. Res. A* **389**, 81 (1997).

[28] H. Morinaga and T. Yamazaki *In-Beam Gamma-ray Spectroscopy* (North-Holland Publishing Company, Amsterdam, New York, and Oxford, 1976).

[29] F. G. Kondev, G. D. Dracoulis, and T. Kibédi, *At. Data Nucl. Data Tables* **103**, 50 (2015).

[30] S. Saha, R. Palit, J. Sethi, S. Biswas, and P. Singh, *J. Instrum.* **11**, P03030 (2016).

[31] T. Inakura, H. Imagawa, Y. Hashimoto, S. Mizutori, M. Yamagami, and K. Matsuyanagi, *Nucl. Phys. A* **768**, 61 (2006).

[32] E. Chabanat, P. Bonche, P. Haensel, J. Mayer, and R. Schaeffer, *Nucl. Phys. A* **627**, 231 (1998).